

FLEXURAL BUCKLING OF STRUCTURAL GLASS COLUMNS. INITIAL GEOMETRICAL IMPERFECTION AS A BASE FOR MONTE CARLO SIMULATION

Ondrej PESEK¹, Jindrich MELCHER²

¹Institute of Metal and Timber Structures, Faculty of Civil Engineering, Brno University of Technology
Veveří 331/95, 602 00 Brno, Czech Republic

²Institute of Metal and Timber Structures, Faculty of Civil Engineering, Brno University of Technology
Veveří 331/95, 602 00 Brno, Czech Republic

pesek.o@fce.vutbr.cz, melcher.j@fce.vutbr.cz

DOI: 10.31490/tces-2018-0003

Abstract. In this paper Monte Carlo simulations of structural glass columns are presented. The simulation was performed according to the analytical second order theory of compressed elastic rods. A previous research on shape and size of initial geometrical imperfections is briefly summarized. An experimental analysis of glass columns that were performed for evaluation of equivalent geometrical imperfections is mentioned too.

Keywords

Structural glass, flexural buckling, geometrical imperfections, Monte Carlo simulation, variation coefficient, statistical distribution, Southwell's plot.

1. Introduction

Glass has been established as a material of load carrying members and structures in the end of twentieth century and its importance still grows today (Fig. 1), but European design code for static design of glass structures is still in progress.

Due to slender of glass members it is necessary to check them on stability problems - flexural buckling of columns or lateral torsional buckling of beams or their interaction (flexural - lateral torsional buckling) of beam - columns. Design methods of steel and timber structures are not completely usable for glass structures because of several differences (initial imperfections, brittle behaviour and laminated glass behaviour) [2]. The shape and size of initial geometrical imperfec-

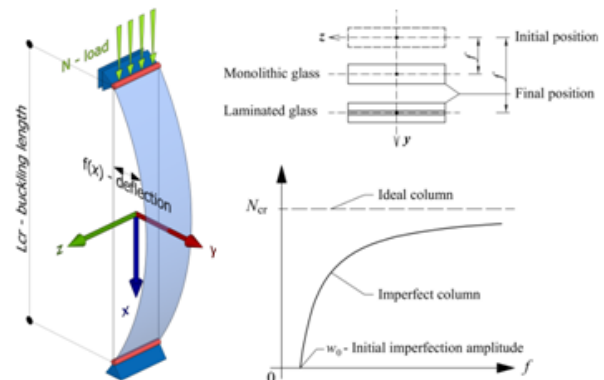


Fig. 1: Flexural buckling of glass column, load-deflection curve of perfect and imperfect member

tions are still poorly published in recent publications; the largest study on this problem was performed by Belis et al. [3]. Pesek and Melcher [4] followed on their work. Behaviour of imperfect columns and beams under load was published in [5]. Equation (1) describe (according to the second order theory) dependency of deformation $f(w_0)_x$ of axially loaded imperfect column on amplitude of initial imperfection. Using equation (2) normal stresses at mid-span can be calculated. Sinusoidal shape of overall bow imperfection is considered in accordance with results of [3] and [4]. Flexural deformation increases with increasing amplitude of initial imperfection.

$$\begin{aligned} f(w_0)_x &= w_0 \frac{N}{N_{cr} - N} \cdot \cos \frac{\pi \cdot x}{L} = \\ &= w_0 \left(\frac{1}{1 - \frac{N}{N_{cr}}} \right) \cdot \cos \frac{\pi \cdot x}{L} \end{aligned} \quad (1)$$

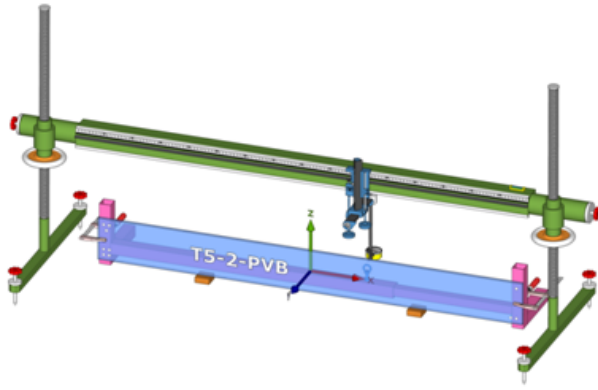


Fig. 2: Carl - Zeiss measuring device

$$\sigma_{max} = \frac{N}{A} \pm \frac{M}{W} = \frac{N}{A} \pm N \cdot w_0 \left(\frac{1}{1 - \frac{N}{N_{cr}}} \right) \quad (2)$$

where:

w_0 - is amplitude of initial geometrical imperfection [mm],

A - section area [mm²],

W - section modulus to weak axis [mm³],

N - normal compressive force [N],

N_{cr} - Euler's critical force [N],

L - column (buckling) length [mm] and

x - point of interest, distance from mid - span [mm].

It is necessary to know size and shape of initial geometrical imperfections to make both types of simulations - analytical simulations according to the second order theory and numerical analysis according to the large deflection theory [6].

Actually there are two types of overall bow imperfection - initial geometrical imperfection (imperfection of unloaded specimen) and equivalent initial geometrical imperfection including three types of imperfections: (i) geometrical imperfections (geometrical curvature of beam or column), (ii) structural imperfections (actual point of load application etc.) and (iii) physical imperfections (residual stresses, inhomogeneity of the material). Equivalent initial geometrical imperfection is a result of Southwell's plot in evaluation of experimental testing. In this paper the both types of geometrical imperfections are mentioned.

The geometrical imperfection of the guiding rail was deducted from measuring the initial shape imperfections of the same glass specimen twice: once in the

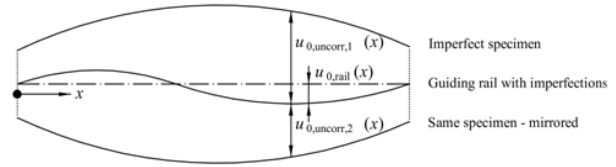


Fig. 3: Determination of guiding rail imperfections

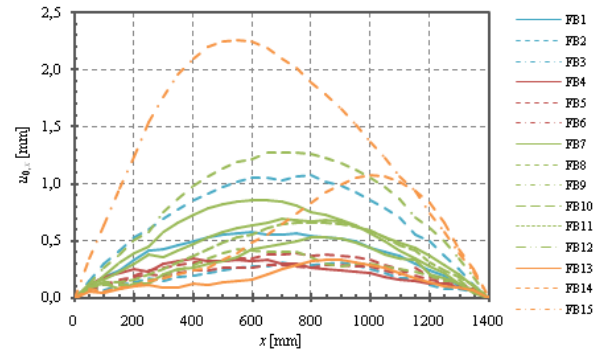


Fig. 4: Determination of guiding rail imperfections

conventional position ($u_0, u_{uncorr,1}$) and once in the mirrored position ($u_0, u_{uncorr,2}$).

Initial geometrical imperfections (global bow) were measured on 33 specimens. Specimens tested on flexural buckling are listed in Tab. 1.

1.1. Shape and Size of Initial Imperfections

Imperfect shapes of specimens tested on flexural buckling are plotted in Fig. 4 where specimens FB1 - FB3 are made of ESG 12, spec. FB4 - FB6 are made of VG 66.2, spec. FB7 - FB12 are made of VSG 66.3 and spec. FB13 - FB15 are made of VSG 444.33. The shapes are mostly symmetrical, only two of them (FB15 and FB14 - both made of laminated safety glass) are significantly asymmetrical. Results of this research were published and discussed in [4] in detail. The biggest initial overall bow imperfection was measured on specimen FB15 - 2.423 mm, which is 1.615 mm/m. The smallest initial overall bow imperfection was measured in specimen FB5 - 0.312 mm, which is 0.208 mm/m. Measured sizes of imperfections confirmed that overall bow imperfections of fully tempered glass are significantly greater than for annealed glass where imperfections are almost negligible. The shapes could be approximated using sinus function and parabola as well. Due to agreement with analytical solution an application of sinus wave is recommended.

Statistical evaluation was carried out in Statistica software [13]. To make summary statistic for all specimens is problematic due to different composition of specimens.

Designation	Description	Glass	Foil	Length [mm]	Width [mm]	Glass thickness [mm]	Foil thickness [mm]
ESG 12	Safety glass	Fully tempered	-	1500	150	12	-
VG 66.2	Laminated glass	Float	PVB	1500	150	6+6	0.76
VSG 66.3	Laminated safety glass	Fully tempered	EVASAFE	1500	150	6+6	1.14
VSG 444.33	Laminated glass	Float	PVB	1500	150	4+4+4	0.76

Tab. 1: The list of measured and tested specimens

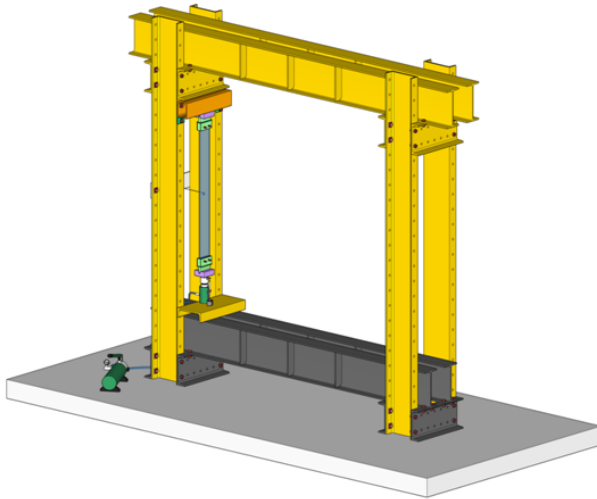


Fig. 5: Determination of guiding rail imperfections

2. EXPERIMENTAL TESTING OF STRUCTURAL GLASS COLUMNS

Tested specimens are listed in Tab. 1.

2.1. Test Set - up

Test set - up is plotted in Fig. 5. Hinged supports were ensured by steel coulters fitted on both ends of specimen. Coulters were equipped with cutting edge which fits into the conical notch of the bearing plate. Timber pads situated between steel coulters and the glass specimen avoided direct contact of the steel and the glass which may cause a failure by local stress concentrations in contacts. The specimen was placed in a steel frame consisting of steel girders and columns. Loading force was generated by manually operated hydraulic press. Loading force, vertical deflection and horizontal (lateral) deflection at mid - span were measured using force transducer, LVDT and wire sensor respectively. Normal stresses at mid - span were measured at selected specimens using strain - gauges glued to sanded glass. Tested specimens were loaded by static force and loading rate was determined by the press cylinder pull (approximately 0.075 mm.s^{-1}).

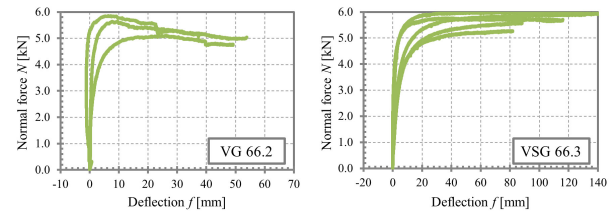


Fig. 6: Force - deflection curves

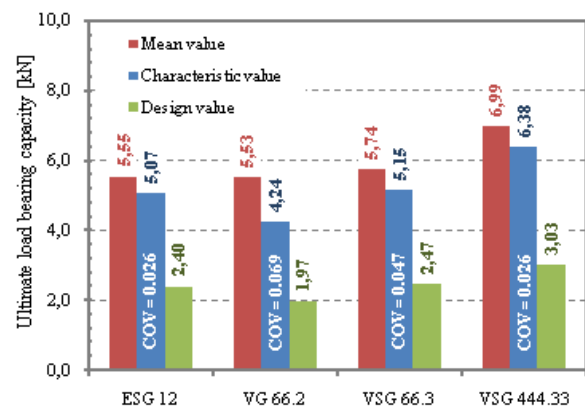


Fig. 7: Statistical evaluation

2.2. Results

Force - lateral deflection curves are plotted in graphs in Fig. 6. Force - lateral deflection curves for all the specimens with the exceptions of laminated double glass with PVB foil (VG 66.2) have an increasing tendency from zero up to failure - it means that the tested specimen was some elastic material [5]. The specimen with PVB foil has curves with decreasing tendency from the point of maximal load - it is characteristic for elastic - plastic materials. Plastic behaviour is caused by PVB foil which has low shear modulus at longer load duration.

Results (ultimate load capacity of each specimen) were statistically evaluated according to the EN 1990 [9], annex D - Design assisted by testing. Calculated mean values, characteristic values and design values are plotted in graph in Fig. 7. Presented values were calculated assuming normal statistical distribution and using equations for unknown variation coefficient.

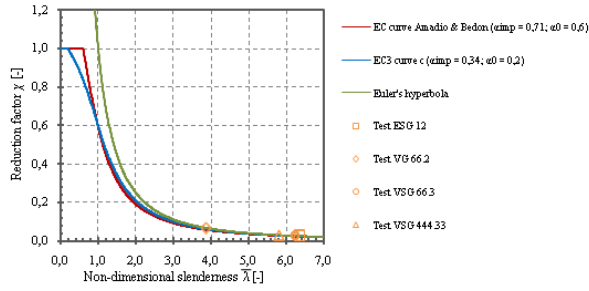


Fig. 8: Buckling curves and reductions factors

2.3. Buckling Curves Approach

The final goal of the research is to develop EC buckling curves (parameters α_{imp} and α_0 that characterizes buckling curve) for simple static design and calculation of buckling resistance $N_{b,Rd}$ - see equations (3)-(5).

$$N_{b,Rd} = \chi \cdot A \cdot f_{g,d} \quad (3)$$

$$\chi = \frac{1}{\Phi + \sqrt{\Phi^2 - \bar{\lambda}^2}} \quad (4)$$

$$\Phi = 0.5 \cdot \left[1 + \alpha_{imp} \cdot (\bar{\lambda} - \alpha_0) + \bar{\lambda}^2 \right] \quad (5)$$

where:

A - is cross section area [mm²],

$f_{g,d}$ - design value of glass tensile strength [MPa],

χ - reduction factor [-] and

$\bar{\lambda}$ - non-dimensional slenderness [-].

In Fig. 8 buckling curve according to Amadio and Bedon [10], [11] and EC3 [12] curve are plotted. Euler's hyperbola is plotted only for comparison. In the graph results of experiments are plotted by orange marks - reduction factors χ_{test} were calculated using equation (6) where $N_{ult,test}$ is maximal normal force measured during test and N_{Rk} is cross section area A multiplied by the characteristic glass strength $f_{g,k}$.

$$\chi_{test} = \frac{N_{ult,test}}{N_{Rk}} \quad (6)$$

Experimentally determined reduction factors χ_{test} are in all cases higher than reduction factors calculated according to the buckling curves - they are above these curves, in means that calculated buckling resistance is on the safe side.

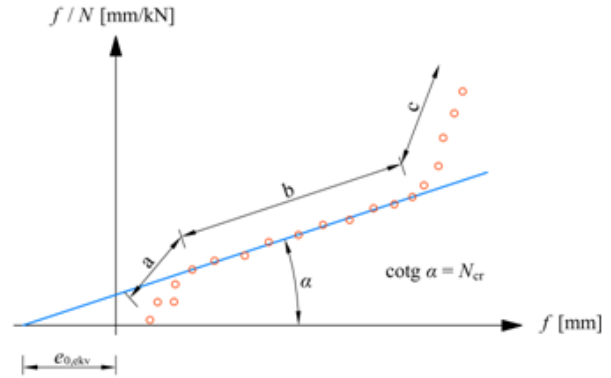


Fig. 9: Southwell's plot

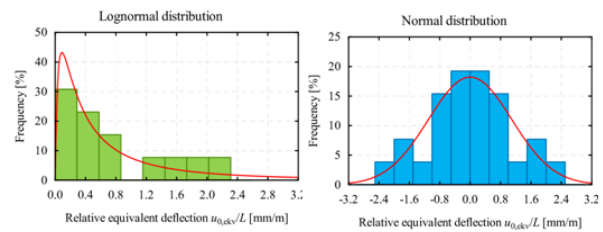


Fig. 10: Histograms for normal and lognormal distribution of equivalent geometrical imperfection

2.4. Equivalent Geometrical Imperfections

It is possible to use Southwell's plot to determine of Euler's critical force N_{cr} and equivalent geometrical initial imperfection $e_{0,ekv}$. Equivalent geometrical imperfection is imperfection that converts all imperfections (geometrical, physical and structural) into one geometrical imperfection. It is convenient because the determination of structural and physical imperfections is difficult and their subsequent application in numerical models or other simulations is problematical.

The principle of Southwell's plot is shown in Fig. 9. Linear function (blue line) is approximated from points only in area b, because of elimination of gaps in test set-up (area a) or plastic states in the end of tests (area c). Calculated equivalent imperfections were statistically evaluated, the mean value of 15 specimens is 1.368 mm (that is 0.818 mm/m) and the imperfection has lognormal distribution - see Fig. 10 on the left. But the recommendation of JCSS [15] is to use normal statistical distribution for geometrical imperfections - histogram for normal distribution of doubled set of measured imperfections is shown in Fig. 10 on the right. 5 % quantiles are 3.591 mm (2.148 mm/m) and 6.665 mm (3.986 mm/m) for normal and lognormal distribution respective. Curvature is approximately $L/250$ in the case of lognormal distribution.

3. Monte Carlo Simulations

In the frame of experimental testing low number of specimens were tested. All tested specimens had extremely high non - dimensional slenderness. From limited results it wasn't possible to verify buckling curves reliably. Monte Carlo simulation offer to verify reliability and accuracy of developed buckling curves for all spectre of non - dimensional slenderness. It requires suitable choice of input parameters.

3.1. Input Parameters

Stochastic values of some input parameters are unavailable; in this case they were estimated. All input parameters for laminated double glass are listed in Tab. 2.

Glass strength $f_{b,kis}$ not a material constant because of fracture behaviour. It depends on size and number of flaws, residual stress, load history, environmental conditions etc. Statistical distribution is best fitted by two - parameter Weibull distribution [14], but these parameters are not presented. Lognormal distribution was used for simplification. Mean value and standard deviation were determined so that 5% quantile is 120 MPa - characteristic value for fully tempered glass. Mean and standard deviation of equivalent geometrical imperfection $w_{0,ekv}$ were determined so that 5% quantile is 4 mm/m - that is result of Southwell's plot of experimental testing (exactly it is 3.986 mm/m for lognormal distribution). Glass thickness t_1 and t_2 hasn't unambiguous statistic distribution due to continual float process. The actual histogram is composed and has two or more significant peaks. Each random selection has different distribution shape. Parameters of uniform distribution corresponded with allowable deviation ± 0.2 mm for thickness 6 mm according to the [8]. Parameters of buckling length L_{cr} were determined to get wide spectre of non - dimensional slenderness. Inter layer shear modulus G_{int} has constant value 1.0 MPa.

3.2. Evaluation of the Simulation

Using MS excel 1000 Monte Carlo simulations were carried out. According to the second order theory were calculated deflections and normal stresses in glass columns with random combinations of input parameters - see equations (1) and (2). Ultimate limit state (buckling strength $N_{ult,MC}$) was considered when normal stress exceeds strength of glass. Then reduction factors were calculated according to the equation (6) where $N_{ult,test}$ was replaced by $N_{ult,MC}$. These reduction factors are plotted in graphs in Fig. 11. In graphs buckling curves according Amadio and Bedon (red line [10], [11]; EC3 (orange line) [12] and new proposed by author (blue line) are plotted. Reduction fac-

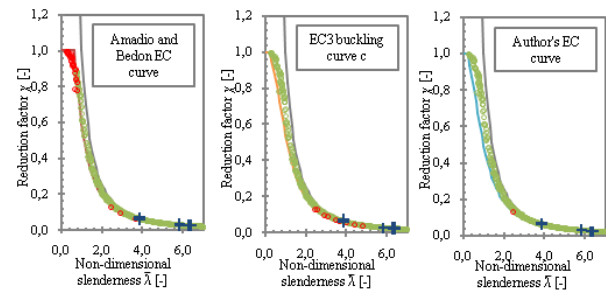


Fig. 11: Monte Carlo simulations results

tors are plotted by red and green colour - green colour is used when reduction factor is above the buckling curve and red colour is used when reduction factor is under buckling curve. In the case of green colour the simulation is on the safe side, in the case of red colour it is on the unsafe side. In graphs Euler's hyperbola is plotted by grey line and blue crosses are reduction factors obtained from experimental testing.

EC3 buckling curve c is conservative for low slender columns, for slenderness from 2.0 to 5.0 there are 9 unsafe cases. Amadio and Bedon buckling curve is unsafe for very low non - dimensional slenderness, where 34 unsafe cases were obtained. Author proposes new curve with parameters listed in Tab. 3 where only 1 case is unsafe, but curve is very uneconomic for slenderness up to 2.0.

4. Conclusions

On basis of experimental testing and measuring of initial imperfections 1000 Monte Carlo simulations were carried out. New buckling curve was developed according to the results of the simulation. Further research should be target to carry out the same simulation using numerical analysis according to the large deflection theory. All simulations could be verified by additional experiments.

Acknowledgment

This paper has been elaborated within the support of the Projects of Czech Ministry of Education, Youth and Sports on Faculty of civil engineering, Brno University of Technology No FAST-S-17-4655.

References

- [1] HALDIMANN, M., LUIBLE, A. and M. OVEREND. *Structural Use of Glass*. 2008, Zurich: ETH Zurich, pp. 215, ISBN 3-85748-119-2.

Tab. 2: The list Monte Carlo simulation input parameters

Variable	Designation	Statistical distribution	Mean	Standard deviation	Variation coefficient
Section width	b	normal	150 mm	0.75 mm	0.005
Interlayer thickness	t_{int}	normal	0.76 mm	0.0038 mm	0.005
Glass Young's modulus	E	normal	70 GPa	3.5 GPa	0.05
Glass tensile strength	$f_{b,k}$	lognormal	5.73 MPa	0.573 MPa	0.1
Amplitude of imperfection	$w_{0,ekv}$	lognormal	1.191 mm	0.119 mm	0.1
			Minimum	Maximum	
Buckling length	L_{cr}	uniform	30 mm	1600 mm	
Glass thickness	$t_1; t_2$	uniform	5.8 mm	6.2 mm	

Tab. 3: Summary of Monte Carlo simulations

Buckling curve	α_0	α_{imp}	Number of unsuitable simulations	P_f
Amadio and Bedon	0.60	0.71	34	0.034
EC3 c	0.20	0.49	9	0.009
author c	0.20	0.65	1	0.001

- [2] PESEK, O., MELCHER, J. and M. HORACEK. Experimental Verification of the Buckling Strength of Structural Glass Columns. *Procedia Engineering*. 2016, Volume 161, pp. 556-562. ISSN 1877-7058, DOI: 10.1016/j.proeng.2016.08.691.
- [3] BELIS, J., MOCIBOB, D., LUIBLE, A. and M. VANDEBROEK. On the size and shape of initial out-of-plane curvatures in structural glass components. Elsevier Ltd. *Construction and Building Materials*. 2011, Volume 25, Issue 5, pp. 2700-2712. ISSN: 0950-0618.
- [4] PESEK, O. and J. MELCHER. Measuring and Evaluation of the Shape and Size of Initial Geometrical Imperfections of Structural Glass Members. *WSEAS Transactions on Applied and Theoretical Mechanics*. 2015, Volume 10, pp. 253-259. ISSN 1991-8747, E-ISSN: 2224-3429.
- [5] BREZINA, V. *Buckling Load Capacity of Metal Rods and Beams (Vzperna unosnost kovovych prutu a nosniku)*. 1962, Prague: Czechoslovak Academy of Science, pp. 384.
- [6] PESEK, O. and J. MELCHER. Numerical analysis of behaviour of compression members made of laminated structural glass. *Transactions of the VSB - Technical University of Ostrava. Construction Series*. December 2013, Volume 23, Issue 2, Pages 117-126, ISSN (Online) 1804-4824, ISSN (Print) 1213-1962, DOI: 10.2478/tvsb-2013-0018.
- [7] EN 1863-1. Glass in building - Heat strengthened soda lime silicate glass - Part 1. *Definition and description*. 2012, Brussel: European Committee for Standardization, pp. 28.
- [8] EN 12150-1. Glass in building - Thermally toughened soda lime silicate glass - Part 1: *Definition and description*. 2001, Brussel: European Committee for Standardization, pp. 24.
- [9] EN 1990. *Eurocode: Basis of structural design*. 2011, Brussel: European Committee for Standardization, pp. 110.
- [10] BEDON, C. and C. AMADIO. Flexural-torsional buckling: Experimental analysis of laminated glass elements. *Elsevier Ltd., Engineering Structures*. 2014, Volume 73, pp. 85-99. ISSN: 0141-0296. DOI: 10.1016/j.engstruct.2014.05.003.
- [11] BEDON, C. and C. AMADIO. A buckling verification approach for monolithic and laminated glass elements under combined in-plane compression and bending. *Elsevier Ltd., Engineering Structures*. 2013, Volume 52, pp. 220-229. ISSN: 0141-0296. DOI: 10.1016/j.engstruct.2013.02.022.
- [12] EN 1993-1-1. *Eurocode 3: Design of steel structures - Part 1-1: General rules and rules for buildings*. 2005, Brussel: European Committee for Standardization, pp. 94.
- [13] StatSoft Inc. STATISTICA ©Cz 12, [software]. Available from: <https://www.statsoft.com>.
- [14] MENCÍK, J. *Strength and fracture of glass and ceramics (Pevnost a lom skla a keramiky)*. 1990, pp. 392 - 986, Prague: State publishing house of technical literature
- [15] JCSS probabilistic model code. The joint committee on structuralsafety [online]. 2001 [cit. 2014-12-15]. Available from: <https://www.jcss.byg.dtu.dk>